The Journal of Immunology

Bach2 Promotes B Cell Receptor–Induced Proliferation of B Lymphocytes and Represses Cyclin-Dependent Kinase Inhibitors

Yuichi Miura, Mizuho Morooka, Nicolas Sax, Rahul Roychoudhuri, Ari Itoh-Nakadai, Andrey Brydun, Ryo Funayama, Keiko Nakayama, Susumu Satomi, Mitsuyo Matsumoto, Kazuhiko Igarashi and Akihiko Muto

J Immunol 2018; 200:2882-2893; Prepublished online 14 March 2018;
doi: 10.4049/jimmunol.1601863
http://www.jimmunol.org/content/200/8/2882

The Journal of Immunology is published twice each month by
The American Association of Immunologists, Inc.,
1451 Rockville Pike, Suite 650, Rockville, MD 20852

Print ISSN: 0022-1767 Online ISSN: 1550-6606.

Bach2 Promotes B Cell Receptor–Induced Proliferation of B Lymphocytes and Represses Cyclin-Dependent Kinase Inhibitors

Yuichi Miura,*,† Mizuho Morooka,* Nicolas Sax,* Rahul Roychoudhuri,‡ Ari Itoh-Nakadai,*,1 Andrey Brydun,* Ryo Funayama,§ Keiko Nakayama,§ Susumu Satomi,† Mitsuyo Matsumoto,* Kazuhiko Igarashi,*,¶,‖ and Akihiko Muto*,¶

BTB and CNC homology 2 (Bach2) is a transcriptional repressor that is required for the formation of the germinal center (GC) and reactions, including class switch recombination and somatic hypermutation of Ig genes in B cells, within the GC. Although BCR-induced proliferation is essential for GC reactions, the function of Bach2 in regulating B cell proliferation has not been elucidated. In this study, we demonstrate that Bach2 is required to sustain high levels of B cell proliferation in response to BCR signaling. Following BCR engagement in vitro, B cells from *Bach2*-deficient (*Bach2*$^{-/-}$) mice showed lower incorporation of BrdU and reduced cell cycle progression compared with wild-type cells. *Bach2*$^{-/-}$ B cells also underwent increased apoptosis, as evidenced by an elevated frequency of sub-G_1 cells and early apoptotic cells. Transcriptome analysis of BCR-engaged B cells from *Bach2*$^{-/-}$ mice revealed reduced expression of the antiapoptotic gene *Bcl2l1* encoding Bcl-x_L and elevated expression of cyclin-dependent kinase inhibitor (CKI) family genes, including *Cdkn1a*, *Cdkn2a*, and *Cdkn2b*. Reconstitution of Bcl-x_L expression partially rescued the proliferation defect of *Bach2*$^{-/-}$ B cells. Chromatin immunoprecipitation experiments showed that Bach2 bound to the CKI family genes, indicating that these genes are direct repression targets of Bach2. These findings identify Bach2 as a requisite factor for sustaining high levels of BCR-induced proliferation, survival, and cell cycle progression, and it promotes expression of Bcl-x_L and repression of CKI genes. BCR-induced proliferation defects may contribute to the impaired GC formation observed in *Bach2*$^{-/-}$ mice. ***The Journal of Immunology*****, 2018, 200: 2882–2893.**

Hematopoietic cells are estimated to constitute >90% of the total 3×10^{13} cells in the human body (1, 2). To fulfill this demand, they undergo massive proliferation along distinct differentiation trajectories from hematopoietic stem cells. Proliferation of hematopoietic cells is strictly controlled, occurring at only specific stages of differentiation along each cell lineage (3). For example, within the B cell lineage, pre-B cells undergo vigorous proliferation to expand cells containing rearranged IgH genes (4), whereas resting mature B cells resume proliferation upon Ag encounter to expand clones that are reactive to that Ag (5).

B cells participate in the elimination of invading microorganisms by producing Abs with high affinity and diverse functions. This is accomplished by somatic hypermutation (SHM) and class switch recombination (CSR) of Ab genes, respectively (6). The BCR is a complex of the transmembrane form of Ig with the heterodimer of Igα/Igβ (7). In mature B cells, Ag binding to the BCR triggers intracellular signaling, inducing B cell activation. Follicular (FO) B cells, a subset of mature B cells, differentiate into germinal center (GC) B cells within GCs where B cells undergo rounds of proliferation, accompanied by SHM and CSR (8–10). DNA damage response, including activation of cell cycle checkpoints, is induced during CSR (11, 12), which may be accompanied by transient cell cycle arrest. Simultaneously, induction of apoptosis in response to DNA damage is suppressed for successful SHM and CSR (13, 14). Following SHM, high-affinity B cells are selected to

*Department of Biochemistry, Tohoku University Graduate School of Medicine, Sendai 980-8575, Japan; †Division of Advanced Surgical Science and Technology, Tohoku University Graduate School of Medicine, Sendai 980-8575, Japan; ‡Laboratory of Lymphocyte Signalling and Development, The Babraham Institute, CB22 3AT Cambridge, United Kingdom; §Department of Cell Proliferation, United Center for Advanced Research and Translational Medicine, Tohoku University Graduate School of Medicine, Sendai 980-8575, Japan; ¶Center for Regulatory Epigenome and Diseases, Tohoku University Graduate School of Medicine, Sendai 980-8575, Japan; and ‖AMED-CREST, Japan Agency for Medical Research and Development, Tokyo 100-0004, Japan

[1]Current address: Department of Experimental Immunology, Institute of Development, Aging and Cancer, Tohoku University, Sendai, Japan.

ORCIDs: 0000-0002-4610-6869 (Y.M.); 0000-0003-4678-1984 (M. Morooka); 0000-0002-2470-2475 (K.I.).

Received for publication November 3, 2016. Accepted for publication February 20, 2018.

This work was supported by Grants-in-Aid (15H02506, 25670156, 24390066, 23116003, 21249014, 17054028, 16K08572, and 25460352) and the Network Medicine Global-COE Program from the Ministry of Education, Culture, Sports, Science and Technology of Japan and by grants from the Uehara Foundation, the Takeda Foundation, the NOVARTIS Foundation (Japan) for the Promotion of Science, the Astellas Foundation for Research on Metabolic Disorders, and the Naito Foundation. R.R. is supported by the Wellcome Trust/Royal Society (Grant 105663/Z/14/Z), the UK Biotechnology and Biological Sciences Research Council (Grant BB/N007794/1), and Cancer Research UK (Grant C52623/A22597).

The Gene Ontology data presented in this article have been submitted to the National Center for Biotechnology Information Gene Expression Omnibus (https://www.ncbi.nlm.nih.gov/geo/query/acc.cgi?acc=GSE103982) under accession number GSE103982.

Address correspondence and reprint requests to Dr. Akihiko Muto, Tohoku University Graduate School of Medicine, Seiryo-machi 2-1, Aoba-ku, Sendai, Miyagi 980-8575, Japan. E-mail address: mutoa@med.tohoku.ac.jp

The online version of this article contains supplemental material.

Abbreviations used in this article: 7-AAD, 7-aminoactinomycin D; Bach2, BTB and CNC homology 2; CDK, cyclin-dependent kinase; ChIP, chromatin immunoprecipitation; ChIP-seq, ChIP followed by sequencing; CKI, CDK inhibitor; CSR, class switch recombination; FO, follicular; GC, germinal center; GO, Gene Ontology; NRS, normal rabbit serum; PC, plasma cell; RT-qPCR, quantitative RT-PCR; SHM, somatic hypermutation; WT, wild-type.

proliferate on the basis of their affinity for the Ag, expanding high-affinity B cell clones in the GC (15). Upon successful completion of these events, B cells undergo terminal differentiation into Ab-secreting plasma cells (PCs) and cease to proliferate (16). Similar to many other cell types, the proliferation of B cells is controlled by cell cycle regulators, such as cyclin, cyclin-dependent kinases (CDKs), and CDK inhibitors (CKIs) (17). We hypothesized that B cells harbor mechanisms ensuring cell type–specific and temporal control of these ubiquitous regulators of the cell cycle and apoptosis.

The transcription factor BTB and CNC homology 2 (Bach2) regulates the differentiation and responses of acquired and innate immune cells at multiple points (18). In particular, Bach2 controls the initiation of B cell differentiation (19), B cell activation (20, 21), T cell differentiation (22–26), and differentiation of tissue-resident macrophages (27, 28). Salient features of Bach2 relevant to this study are as follows. Bach2 is required for SHM, CSR, GC formation, and inhibition of PC differentiation (20, 21). A part of these requirements may be explained by the repression of *Prdm1*, which encodes the PC transcription factor Blimp-1, by Bach2 (29–31). Importantly, Bach2 is phosphorylated by the PI3K–Akt–mTOR pathway in response to BCR signaling (32). Because the PI3K–Akt–mTOR pathway regulates proliferation and survival of mature B cells in response to BCR activation (33–37), Bach2 may regulate genes required for proliferation and/or survival. Several reports have implicated *Bach2* overexpression in the pathogenesis of B cell lymphoma in humans and mouse models (38–41), suggesting its role in the regulation of proliferation and/or apoptosis. These findings prompted us to test the hypothesis that Bach2 is required for B cell proliferation. We found that Bach2 is indispensable for BCR-induced proliferation; it promotes survival and cell cycle progression via upregulation of Bcl-x_L and repression of CKI genes, respectively.

Materials and Methods

Mice

The establishment of *Bach2*$^{-/-}$ mice was described previously (20). All animal studies were approved by the Institutional Animal Care and Use Committee of the Tohoku University Environmental and Safety Committee.

FO B cell sorting

Splenocytes were stained with fluorescent dye–conjugated Abs specific for CD19 (1D3), CD21/CD35 (7G6), CD23 (B3B4), and IgM (R6-6002; all from BD Biosciences). FO B cells (CD19$^+$, IgM$^+$, CD21^{low}, and CD23$^+$) were sorted using a FACSAria II (BD Biosciences).

B cell stimulation

Purified B cells were cultured in 12-well plates at 7.5×10^6 cells per well, in 24-well plates at 1.0×10^6 cells per well, and in 96-well plates at 2×10^5 cells per well in RPMI 1640 medium (Sigma) containing anti-mouse IgM [F(ab′)$_2$] (115-006-020; Jackson ImmunoResearch Laboratories), LPS (0111:B4; Sigma) or rCD40L (8230; R&D Systems) at the indicated concentrations for the indicated times.

Proliferation analysis

Proliferation of stimulated FO B cells was determined by measurement of DNA synthesis through addition of BrdU during the last 6 h of culture. After BrdU treatment, cells were fixed and incubated with peroxidase-conjugated anti-BrdU Ab, followed by addition of substrate, according to the manufacturer's protocol (Cell Proliferation ELISA, BrdU Kit; Roche). Absorbance at 450 nm was measured using a microplate reader (Bio-Rad).

B cell purification

Splenic B cells were purified by mouse CD45R (B220) MicroBeads or a B Cell Isolation Kit, mouse (Miltenyi Biotec). The purity of isolated cells was typically 90%.

Cell cycle analysis

Cell cycle progression of stimulated splenic B cells was determined by measurement of DNA synthesis and DNA contents by BrdU incorporation and 7-aminoactinomycin D (7-AAD) staining, respectively (BD Biosciences). Stimulated splenic B cells were supplemented with BrdU for the last 45 min of culture. Following BrdU treatment, cells were fixed with formaldehyde and permeabilized with saponin. Then, cells were incubated with 300 μg/ml DNase I for 1 h at 37°C, followed by incubation with FITC-conjugated anti-BrdU Ab for 20 min at room temperature. The cells were resuspended in 7-AAD–containing PBS and analyzed using a FACSCalibur (BD Biosciences).

Apoptotic cells detection

The frequency of apoptotic cells in stimulated splenic B cells was measured by annexin V binding to phosphatidylserine on the outer cell membrane and permeability of 7-AAD through the cell membrane. After stimulation, cells were washed with PBS and resuspended in Annexin V Binding Buffer (BD Biosciences) at 1×10^6 cells per milliliter, stained with FITC Annexin V (BD Biosciences) and 7-AAD for 15 min at room temperature in the dark, and analyzed using a FACSCalibur or FACSVerse (BD Biosciences).

Active caspases detection

To analyze the status of active caspases in cultured B cells, cells were incubated with zVAD–FMK–fluorescein for 45 min at 37°C with 5% CO_2 and washed twice, according to the manufacturer's protocol (CaspGLOW Fluorescein Active Caspase Staining Kit; eBioscience).

Immunoblot analysis

Protein extraction from splenic B cells was carried out with radioimmunoprecipitation assay buffer (30). The cell extracts were separated by electrophoresis on SDS-polyacrylamide gel. Following SDS-PAGE, the proteins were electrotransferred to a PVDF Membrane (Millipore). The membrane was blocked for 1 h in blocking buffer (TBS supplemented with 0.05% Tween 20 and 5% BSA) and then incubated with primary and secondary Abs in blocking buffer for 8 h and 30 min, respectively. Detection of immunoreactive proteins was carried out using ECL Western Blotting Detection Reagent (GE Healthcare) or Pierce ECL Plus Western Blotting Substrate (Thermo Fisher Scientific). The following Abs were used for immunoblotting: anti–phospho-Syk Ab (#2701), anti-Syk Ab (#2712), anti–phospho-MEK1/2 Ab (#9121), anti-MEK1/2 Ab (#4694), anti–phospho-Erk1/2 Ab (#9101), anti-Erk1/2 Ab (#9102), anti–phospho-Akt Ab (#9271), anti-Akt Ab (#9272), anti–phospho-p38 Ab (#9211), anti-p38 Ab (#9212), anti–phospho-IκBα Ab (#2859), anti-IκBα Ab (#9247; all from Cell Signaling Technology), anti–α-tubulin Ab (sc-5286), and anti–NF-κB p52 (sc-7368; both from Santa Cruz Biotechnology). ECL anti-Rabbit IgG (NA934V) and ECL anti-Mouse IgG (NA931V; both from GE Healthcare) were used as secondary Abs.

RT-PCR

RNA was prepared from B cells using a Total RNA Isolation Mini Kit (Agilent Technologies) or an RNeasy Plus Mini Kit (QIAGEN). cDNA was synthesized using an Omniscript RT Kit (QIAGEN) with Random Hexamers (Invitrogen). For quantitative PCR, LightCycler FastStart DNA Master SYBR Green I reagents and a LightCycler system (both from Roche) were used. The following PCR primers were used: *Bcl2l1*: forward 5′-GTTGGATGGCCACCTATCTG-3′ and reverse 5′-TGTCTGGTCACTTCCGACTG-3′, *Bcl2*: forward 5′-TCGCTACCGTCGTGACTTC-3′ and reverse 5′-AAACAGAGGTCGCATGCTG-3′, *Bcl2l2*: forward 5′-GGACAAGTGCAGGATTGGAT-3′ and reverse 5′-TCCCCGTATAGAGCTTGTGAA-3′, *Mcl1*: forward 5′-CTTGTAAGGACGAAACGG-3′ and reverse 5′-AAGAGTCCCCTATTGCAC-3′, *Bbc3*: forward 5′-ATGGCGGACGACCTCAAC-3′ and reverse 5′-AGTCCCATGAAGAGATTGTACATGAC-3′, *Bcl2l11*: forward 5′-CCCGGAGATACGGATTGCAC-3′ and reverse 5′-GCCTCGCGGTAATCATTTGC-3′, *Bid*: forward 5′-AATCATCCACAACATTGCCAGA-3′ and reverse 5′-GCCTTGTCGTTCATGTCT-3′, *Bbc2*: forward 5′-CTCCGAAGGATGAGCGATGAG-3′ and reverse 5′-TGGTCGCATCTGTGTTGCAGT-3′, *Pmaip1*: forward 5′-GTGCACCGGACATAACTG-3′ and reverse 5′-AGCACACTCGTCCTTCAAG-3′, *Bax*: forward 5′-TGAAGACAGGGGCCTTTTTG-3′ and reverse 5′-AATTCGCCGGAGACACTCG-3′, *Bak1*: forward 5′-CAACCCCGAGATGGACAACTT-3′ and reverse 5′-CGTAGCGCCGGTTAATATCAT-3′, *Ccnd1*: forward 5′-GGCGTACCCACAGAAACCAT-3′ and reverse 5′-GCGGTTTCAGATCACGATGC-3′, *Ccnd2*: forward 5′-GCCAAGATCACCCACACTGA-3′ and reverse 5′-GCGTTATGCTGCTCTTGACG-3′, *Ccne1*: forward 5′-ACTTTCTGCAGCGTCATCCT-3′ and reverse 5′-GAACGTCTCTCTGTGGAGCTT-3′, *Cdk2*: forward

5′-CCTGAAATTCTTCTGGGCTGC-3′ and reverse 5′-CATGGTGCTGGGTACACACT-3′, *Cdk4*: forward 5′-CGCGGCCTGTGTCTATGGT-3′ and reverse 5′-ATTCTCGAAGCAGGGGATCTTAC-3′, *Cdk6*: forward 5′-GGCGTACCCACAGAAACCAT-3′ and reverse 5′-GCGGTTTCAGATCACGATGC-3′, *Cdk8*: forward 5′-TGAGAGTTGTCCCTCCTACCA-3′ and reverse 5′-GATGTGCTTGGTCCAGGGTT-3′, *Cdk10*: forward 5′-GGGCCTATGGTGTTCCAGTAA-3′ and reverse 5′-ATGCTGGTAGTCTGGGTGGTA-3′, *Cdkn1a*: forward 5′-GCAGATCCACAGCGATATCCA-3′ and reverse 5′-AGACAACGGCACACTTTGCT-3′, *Cdkn1b*: forward 5′-GGACCAAATGCCTGACTCGT-3′ and reverse 5′-GGCCCTTTTGTTTTGCGAAGA-3′, and *Cdkn2a*: forward 5′-GCTCTGGCTTTCGTGAACA-3′ and reverse 5′-TCGAATCTGCACCGTAGTTG-3′. The primers for β-actin mRNA (*Actb*) were acquired from Nihon Gene Research Laboratories.

DNA microarray analysis

RNA samples were labeled using a Low Input Quick Amp Labeling Kit, according to the manufacturer's protocol, and were hybridized on Mouse Gene Expression 4×44K microarray slides (both from Agilent Technologies). Signals on microarray slides were scanned by an Agilent G2565CA Microarray Scanner System (Agilent Technologies). Acquired data were normalized and filtered on the error coefficient of variation < 50% using GeneSpring software (Agilent Technologies). k-means clustering of the filtered data was performed in R (https://www.r-project.org). The Tukey HSD test (TukeyHSD function in R) was adopted for assessment of the significant difference of averages in each cluster. The heat maps and box plots were created by the ComplexHeatmap 1.6.0 and boxplots packages of R, respectively. Gene Ontology (GO) analysis was performed using DAVID Bioinformatics Resources (42). The data presented in this article have been submitted to the National Center for Biotechnology Information Gene Expression Omnibus under accession number GSE103982 (https://www.ncbi.nlm.nih.gov/geo/query/acc.cgi?acc=GSE103982).

Chromatin immunoprecipitation assay

Chromatin fixation and immunoprecipitation were carried out using the BAL17 mature B cell line or splenic B cells, as previously described (29). In brief, BAL17 cells were fixed with 1% formaldehyde, followed by quenching with 125 mM glycine. The cells were washed with ice-cold PBS and lysed. The cross-linked chromatin was sheared with a Bioruptor Sonicator (Cosmo Bio). Chromatin immunoprecipitation (ChIP) was performed using anti-Bach2 antiserum and normal rabbit serum (NRS; Jackson ImmunoResearch) as a control. Genomic DNA was isolated using a DNA Clean and Concentrator Kit (Zymo Research), according to the manufacturer's protocol. Relative immunoprecipitation efficiency, expressed as the ratio between immunoprecipitated samples and input, was measured by quantitative PCR (Roche). The following PCR primers were used: Region 1: forward 5′-GGAGCTGGAAGATCCCACAC-3′ and reverse 5′-AGTCACCCGACAGGATGAGA-3′, Region 2: forward 5′-ATCGTGACGTGTTTTGTGGC-3′ and reverse 5′-CCAAAACTGCTTGGGCACC-3′, Region 3: forward 5′-GGAAGGTCTGATGAGGGTGC-3′ and reverse 5′-AGGCCGTCTGATCAGCAAAA-3′, and Region 4: forward 5′-GAAAGGTCAGCAACCTACTTGTG-3′ and reverse 5′-GATGACTCAGCAAAAAGCCAGT-3′.

ChIP followed by sequencing

ChIP followed by sequencing (ChIP-seq) libraries were prepared from ∼3 ng of the immunoprecipitated DNA using an Ovation Ultralow DR Multiplex System 1–8 (0330-32; NuGEN). The libraries were clonally amplified on a flow cell and sequenced on HiSeq 2500, controlled by sequence control software v2.0.12, with 51-mer paired end sequence (Illumina). Image analysis and base calling were performed using real-time analysis software (RTA v1.17.21.; Illumina). Hypergeometric tests were conducted to assess the statistical significance using the phyper function of R. The accession number for the ChIP-seq data is GSE87503 (https://www.ncbi.nlm.nih.gov/geo/query/acc.cgi?acc=GSE87503).

Retroviral infection

The retrovirus vector pMSCV Bcl-x_L–IRES–EGFP was generated by PCR from FLAG sequence fused *Bcl2l1* cDNA using an XhoI site–containing forward primer (5′-CCG*CTCGAG*ATGGACTACAAGGACGACGATGAC-3′) and an XhoI site–containing reverse primer (5′-CCG*CTCGAG*TCACTTCCGACTGAAGAGTGAGCC-3′). The fragment was inserted into the XhoI site of pMSCV–IRES–EGFP (43). PlatE virus packaging cells were transfected with each expression vector using FuGENE HD transfection reagent (Promega); the viral supernatants were harvested 2 and 3 d after transfection and used to infect LPS-activated splenic B cells from wild-type (WT) or *Bach2*$^{-/-}$ mice.

Statistical analysis

Statistical significance was estimated using the unpaired two-tailed Student *t* test.

Results

Arrest of cell cycle progression of Bach2$^{-/-}$ *B cells upon BCR signaling*

Because GC B cells show higher expression of Bach2 (44–46) and are dependent on Bach2, we analyzed the proliferative response of *Bach2*-deficient (*Bach2*$^{-/-}$) FO B cells to mitogenic stimulation. WT FO B cells showed a dose-dependent increase in BrdU incorporation in response to BCR engagement with anti-IgM Ab. In contrast, *Bach2*$^{-/-}$ FO B cells exhibited significantly reduced incorporation of BrdU, regardless of the concentrations of the anti-IgM Ab (Fig. 1A). Consistent with our previous observations (20), proliferation in response to LPS was not affected by the loss of Bach2 (Fig. 1A). Therefore, the observed impairment in proliferation was not caused by a universal defect in DNA synthesis or cell cycle progression in *Bach2*$^{-/-}$ FO B cells. To investigate whether impaired BrdU incorporation of *Bach2*$^{-/-}$ B cells was accompanied by cell cycle arrest, we quantified cell cycle progression by flow cytometry. CD45R-expressing (B220$^+$) splenic B cells consist of FO B cells, marginal zone B cells, and transitional B cells. Because we observed a similar reduction in proliferation when using B220$^+$ splenic B cells (Fig. 1B), we chose to use B220$^+$ splenic B cells in the subsequent experiments. In addition to Ag stimulation, GC B cells receive proliferative and survival signals via CD40 from FO Th cells, prompting us to test whether CD40 signaling could rescue the proliferative defect in *Bach2*$^{-/-}$ B cells. A decrease in proliferation was observed in *Bach2*$^{-/-}$ B cells in response to IgM with CD40 stimulation (Supplemental Fig. 1A). *Bach2*$^{-/-}$ B cells failed to enter the S phase, and most of the cells remained in the G_0/G_1 phase, whereas WT B cells efficiently entered the S phase after 48 h of BCR engagement (Fig 1C, 1D). Additionally, a slight increase in the sub-G_1 fraction was observed in *Bach2*$^{-/-}$ B cells (Fig 1C, 1D). *Bach2*$^{-/-}$ B cells also showed a reduced entry into the S phase upon LPS stimulation, although it was of a lesser magnitude than that following BCR engagement. In contrast with BCR engagement, LPS did not induce apoptosis in these cells judging from the numbers of cells in the sub-G_1 fraction (Fig 1C, 1D). Therefore, *Bach2*$^{-/-}$ B cells failed to enter the cell cycle and underwent increased apoptosis in response to BCR signaling. These observations indicate that Bach2 is required for cell cycle progression beyond the G_1/S checkpoint and suggest that Bach2 suppresses apoptosis in response to BCR signaling.

Increased apoptosis of Bach2$^{-/-}$ *B cells upon BCR signaling*

To investigate the role of Bach2 in B cell survival in response to BCR signaling, we compared the frequency of apoptotic cells by staining with annexin V and 7-AAD, which bind to phosphatidylserine exposed by apoptotic cells and DNA exposed upon loss of integrity of the cytoplasmic membrane, respectively (Fig. 2A). Flow cytometric analysis of BCR-engaged *Bach2*$^{-/-}$ B cells revealed a markedly increased frequency of annexin V$^+$7-AAD$^-$ cells, known as early apoptotic cells (47), compared with WT B cells (Fig. 2A). Moreover, we examined cell survival by annexin V binding of BCR-engaged FO B cells from these mice. The fraction of annexin V$^+$ cells in *Bach2*$^{-/-}$ and WT FO B cells was 52.57 ± 4.8% and 70.30 ± 8.1%, respectively, confirming that *Bach2*$^{-/-}$ B cells undergo increased apoptosis when similar starting populations are subjected to BCR signaling. Consistent with the cell cycle analysis (Fig. 1B, 1C), WT and *Bach2*$^{-/-}$ B cells showed a comparable frequency of early apoptotic cells in response to LPS signaling (Fig. 2A).

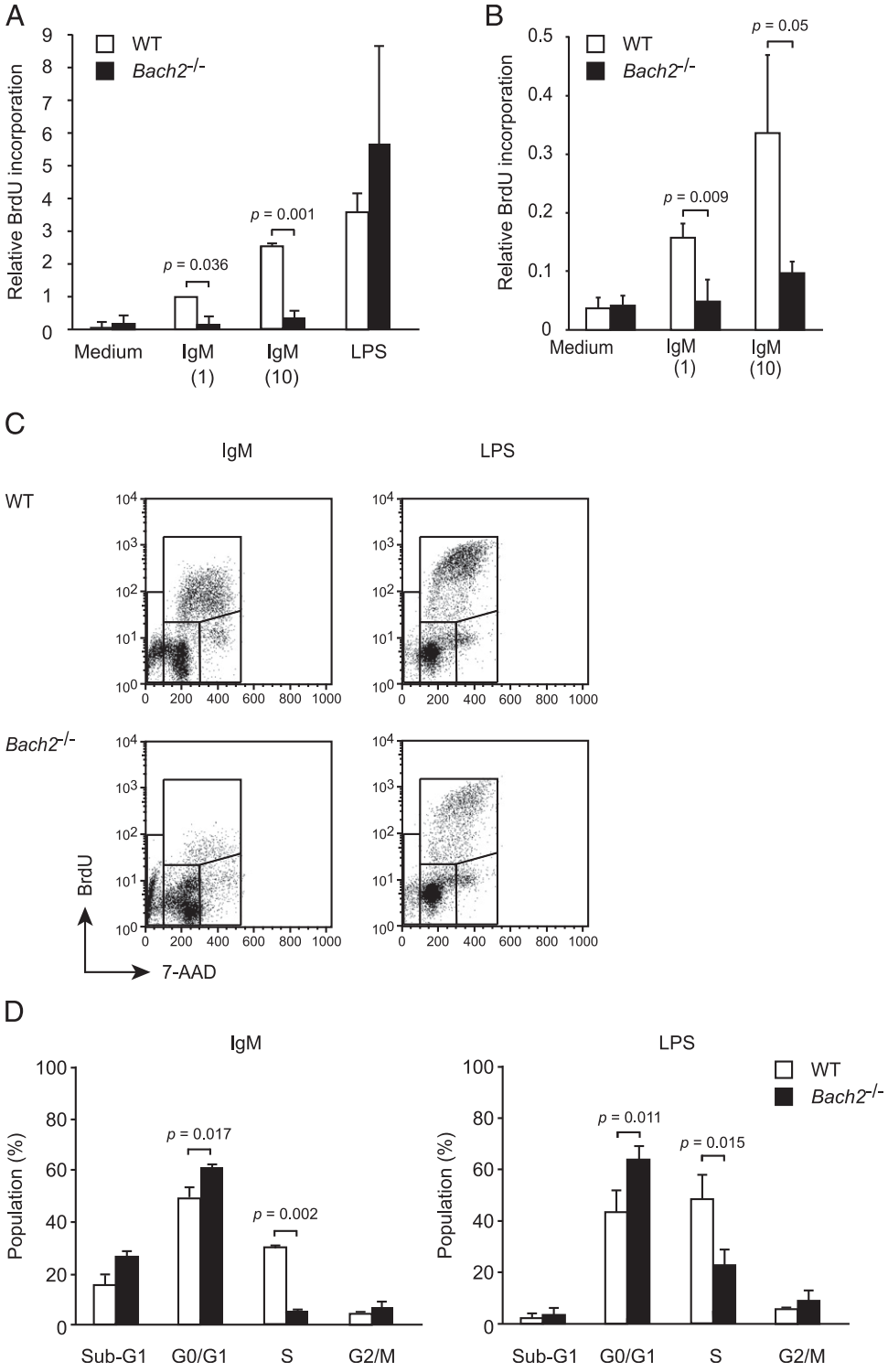

FIGURE 1. Decreased proliferative response in *Bach2*$^{-/-}$ B cells in response to BCR signaling. Purified FO B cells (**A**) or purified CD45R-expressing (B220^{+}) B cells (**B**) from WT and *Bach2*$^{-/-}$ mice were cultured with anti-IgM Ab (1, 10 μg/ml) or LPS (20 μg/ml) for 48 h, and BrdU for the last 6 h, followed by measurement of BrdU incorporation. Data are the mean ± SD of three independent experiments. The proportions of BrdU incorporation were calculated relative to that of WT B cells cultured with 1 μg/ml anti-IgM Ab. Numbers in parentheses indicate the concentration of anti-IgM Ab (μg/ml). (**C**) Representative FACS plots of DNA contents (7-AAD) and DNA synthesis (BrdU). Purified splenic B cells from WT and *Bach2*$^{-/-}$ mice were cultured with 10 μg/ml anti-IgM Ab or 20 μg/ml LPS for 48 h and BrdU for the last 45 min. (**D**) Percentages of cells in the sub-G_1, G_0/G_1, S, and G_2/M phases within WT and *Bach2*$^{-/-}$ splenic B cells. Data are the mean + SD of three independent experiments. The *p* values were determined using a Student *t* test.

Caspases are a family of intracellular cysteine proteases that plays a central role in the initiation and execution of apoptosis (48). To investigate whether excessive induction of apoptosis in *Bach2*$^{-/-}$ B cells upon BCR signaling was associated with caspases, we assessed caspase activity using an FITC-conjugated caspase inhibitor (FITC–VAD–FMK) as a probe (49). Upon stimulation of WT B cells with BCR engagement or LPS, the cells could be separated into two populations based on staining with FITC–VAD–FMK (Fig. 2B). When *Bach2*$^{-/-}$ B cells were stimulated by BCR engagement, most cells were in the fraction with activated caspase (Fig. 2B). In contrast, a substantial portion of the cells remained in the fraction without activated caspase when *Bach2*$^{-/-}$ B cells were stimulated with LPS. These results suggest that Bach2 is required to suppress apoptosis upon BCR signaling.

PI3K–Akt and MEK–Erk pathways were largely unimpaired in Bach2$^{-/-}$ *B cells*

Impaired cell cycle progression and increased apoptosis in *Bach2*$^{-/-}$ B cells might be caused by defects in the transduction of BCR signaling. To investigate this possibility, we evaluated the phosphorylation levels of Syk, Akt, MEK, Erk1/2, and p38 MAPK in WT and *Bach2*$^{-/-}$ B cells at various time periods after BCR

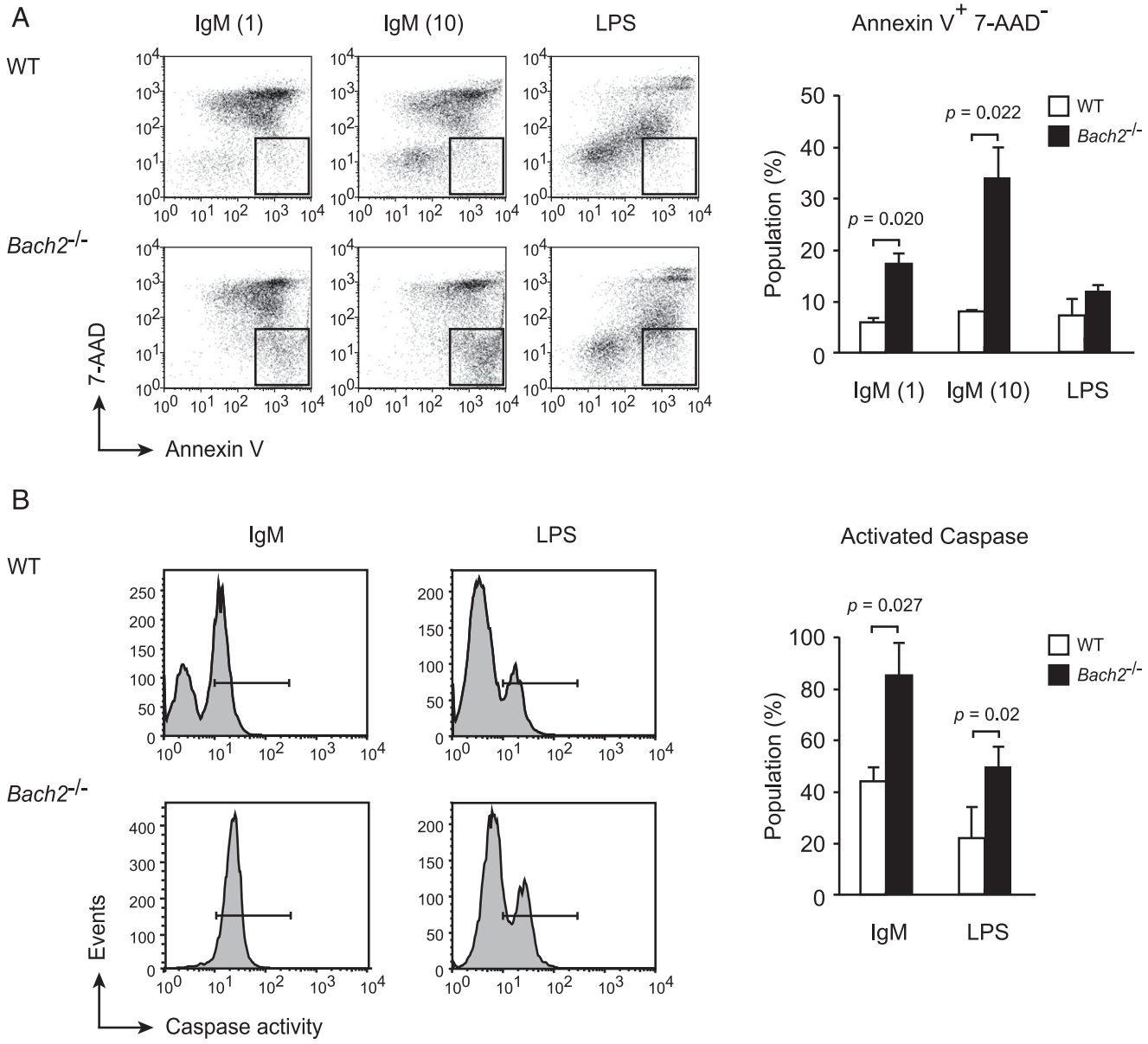

FIGURE 2. Bach2 deficiency resulted in enhanced apoptosis in response to BCR signaling. (**A**) Representative FACS plots of annexin V^+ and 7-AAD^- early apoptotic cells from WT and *Bach2*$^{-/-}$ splenic B cells cultured in the presence of anti-IgM Ab (1, 10 μg/ml) or LPS (20 μg/ml) for 48 h (left panels). Percentages of early apoptotic populations, indicated by a box in the FACS plots, are shown as the mean ± SD of three independent experiments (right panel). (**B**) Representative line graphs of flow cytometric analysis show activated caspases of FO B cells detected by the FITC-labeled caspase inhibitor FITC–VAD–FMK, which irreversibly binds to activated caspases in apoptotic cells (left panels). FO B cells were treated for 48 h with 10 μg/ml anti-IgM Ab or 20 μg/ml LPS. Percentages of FITC–VAD–FMK^+ apoptotic cell populations from WT or *Bach2*$^{-/-}$ FO B cells (right panel). Data are the mean + SD of three independent experiments. The *p* values were determined using a Student *t* test.

engagement (Fig. 3). Immunoblot analysis revealed a rapid induction of the phosphorylation of Syk, a proximal signaling component of the BCR, upon BCR engagement of WT B cells (Fig. 3A). In *Bach2*$^{-/-}$ B cells, changes in the levels of phosphorylated Syk appeared similar to those in WT B cells. Phosphorylation of Akt, a downstream component of the PI3K signaling pathway, was similarly induced upon BCR engagement in WT and *Bach2*$^{-/-}$ B cells (Fig. 3B). WT B cells showed elevated phosphorylation of MEK 5 min after BCR engagement that decreased thereafter, whereas *Bach2*$^{-/-}$ B cells showed higher levels of phosphorylation that were sustained for a longer period (Fig. 3A). In contrast, phosphorylation of Erk1/2, located downstream of the MEK signaling pathway, was induced equivalently in WT and *Bach2*$^{-/-}$ B cells, suggesting that sustained phosphorylation of MEK in *Bach2*$^{-/-}$ B cells had no clear influence on the downstream pathway (Fig. 3C). Moreover, phosphorylation of p38 MAPK was not induced in response to BCR signaling in WT or *Bach2*$^{-/-}$ B cells (Fig. 3D). These results indicate that BCR-mediated activation of the PI3K–Akt and MEK–Erk pathways was not grossly impaired in *Bach2*$^{-/-}$ B cells.

Transcriptome and ChIP-seq analyses in Bach2$^{-/-}$ *B cells upon BCR signaling*

These results raised the possibility that transcriptional regulation in response to BCR signaling, rather than the processes of signal transduction itself, might be affected in *Bach2*$^{-/-}$ B cells. To uncover the underlying molecular mechanism of the proliferation defects among *Bach2*$^{-/-}$ B cells, we measured changes in global gene expression in *Bach2*$^{-/-}$ and WT FO B cells in response to BCR signaling. Based on expression values, genes were divided into six clusters (C1–C6) by k-means clustering (Fig. 4A). To

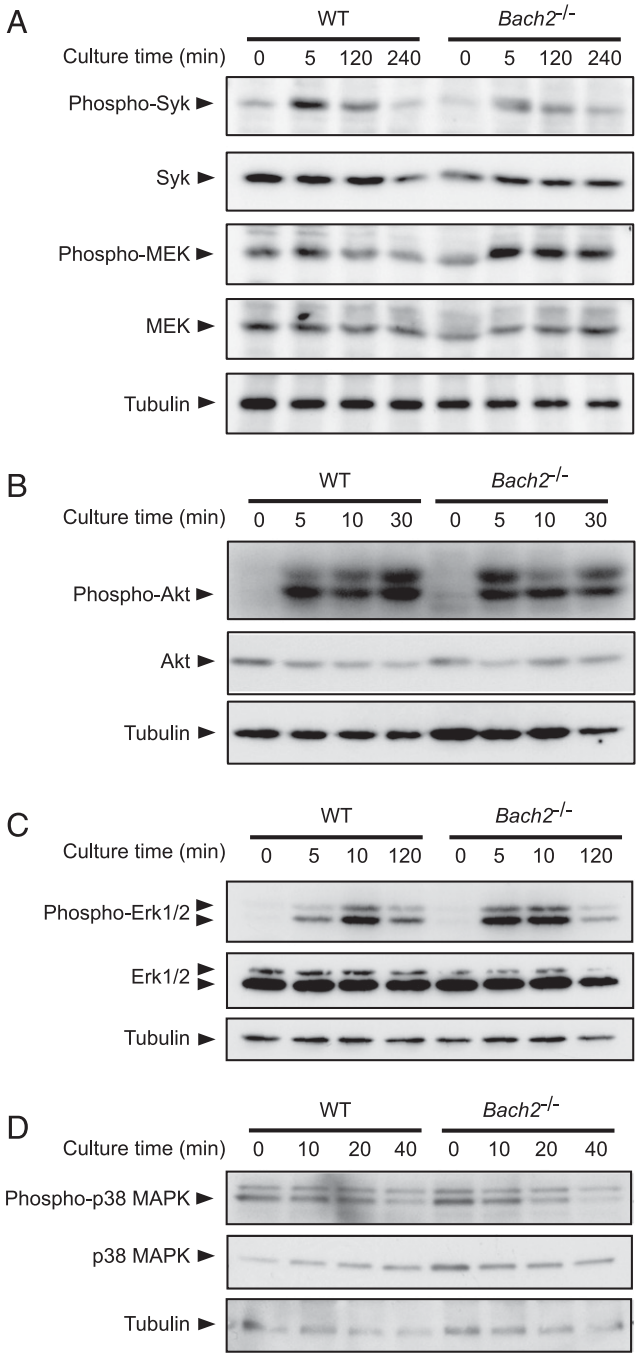

FIGURE 3. Transduction of BCR signaling was unimpaired in *Bach2*$^{-/-}$ splenic B cells. Purified splenic B cells from WT or *Bach2*$^{-/-}$ mice were cultured with 10 μg/ml anti-IgM Ab for the indicated time periods. Whole-cell extracts were subjected to immunoblot analysis to monitor phosphorylated and total amounts of Syk and MEK (**A**), Akt (**B**), Erk1/2 (**C**), and p38 MAPK (**D**). Tubulin serves as a loading control. Data are representative of two or three independent experiments.

identify clusters involving genes whose expression was affected by the loss of Bach2, we compared average gene-expression levels in each cluster using the Tukey HSD test (Fig. 4B). In C2, gene-expression levels in *Bach2*$^{-/-}$ B cells were significantly lower than those in WT B cells without stimulation, whereas there was no differential expression between *Bach2*$^{-/-}$ and WT B cells after BCR engagement. Genes in C3 exhibited increased expression upon BCR engagement and were more highly expressed in *Bach2*$^{-/-}$ B cells. Although genes in C6 were not induced in response to BCR signaling in WT B cells, they showed a strikingly increased expression in the absence of Bach2. Next, to investigate whether Bach2 directly regulates the genes classified into these clusters, we measured genome-wide Bach2 binding in an *Ebf1*$^{-/-}$ pro-B cell line using ChIP-seq (50). We then integrated Bach2 binding and transcriptional data to identify genes putatively targeted by Bach2 directly. A hypergeometric test revealed that the clusters C3, C5, and C6 were substantially enriched in Bach2-bound genes (Fig. 4C). Of particular relevance, clusters C3 and C6 contained genes upregulated in the absence of Bach2 either only in BCR-activated B cells (C3) or in both resting and BCR-activated B cells (C6).

GO term enrichment analysis of each cluster indicated an enrichment in genes involved in the regulation of cell proliferation (GO:0042127) and death (GO:0016265) in the C3 cluster and genes involved in the regulation of apoptosis (GO:0042981) in the C6 cluster (Fig. 4D, Supplemental Table I). To ascertain whether the loss of Bach2 affects the expression levels of all genes assigned to these biological processes, we compared their expression levels in WT and *Bach2*$^{-/-}$ FO B cells stimulated with BCR. Among the genes assigned to regulation of cell proliferation, death, and regulation of cell apoptosis, we found that 19, 17, and 31 genes, respectively, were differentially expressed ≥2-fold in *Bach2*$^{-/-}$ FO B cells in comparison with WT cells. Among these genes, 17, 15, and 31, respectively, were upregulated in *Bach2*$^{-/-}$ FO B cells (Fig. 4D). Notably, combinational analysis of transcriptome and ChIP-seq data revealed that most of the differentially expressed genes in these GO categories were bound by Bach2 (Fig. 4D). These results suggest that Bach2 represses a cohort of genes involved in proliferation and apoptosis in activated B cells.

Downregulation of Bcl-x$_L$ *in* Bach2$^{-/-}$ *B cells upon BCR signaling*

The results of our transcriptional analysis (Fig. 4D) prompted us to evaluate whether *Bach2* deficiency affects the expression of Bcl-2 family members, which function as gatekeepers of apoptosis (51, 52). We examined the transcript levels of anti- and proapoptotic genes by quantitative RT-PCR (RT-qPCR) over time. Among the antiapoptotic genes, expression of *Bcl2l1*, encoding Bcl-x$_L$, increased substantially following BCR engagement in WT B cells. In contrast, *Bach2*$^{-/-}$ B cells showed a weaker induction compared with WT B cells (Fig. 5A), which was consistent with the results in Fig. 4D. Expression of other antiapoptotic genes, such as *Bcl2*, *Bcl2l2*, and *Mcl1*, was not induced in response to BCR signaling, and these genes were not significantly differentially expressed in WT and *Bach2*$^{-/-}$ B cells (Fig. 5A). Among proapoptotic genes, *Bbc3*, encoding Puma, was expressed at significantly higher levels in *Bach2*$^{-/-}$ B cells prior to BCR engagement (Supplemental Fig. 1D). However, its expression was unchanged following BCR engagement, resulting in a level comparable to that in WT B cells. Expression levels of other proapoptotic genes, such as *Bcl2l11*, *Bid*, *Bbc2*, *Pmaip1*, *Bax*, and *Bak*, were not affected by *Bach2* deficiency. By quantitative PCR analysis, a decrease in *Bcl2l1* expression was confirmed in *Bach2*$^{-/-}$ FO B cells compared with WT FO B cells (Supplemental Fig. 2A). Taken together, these results indicate that Bach2 promotes the expression of Bcl-x$_L$ upon BCR signaling.

Because *Bcl2l1* expression is known to be promoted by the CD40 signaling pathway via NF-κB–dependent transcriptional regulation (53), we assessed the activation of canonical and noncanonical NF-κB pathways in CD40-stimulated *Bach2*$^{-/-}$ B cells. An in vitro culture assay demonstrated that the CD40-induced upregulation of both NF-κB pathways was not affected by the loss of Bach2 (Supplemental Fig. 1B, 1C), suggesting that downregulation of *Bcl2l1* expression might not be due to a defect in NF-κB–dependent transcriptional activation in *Bach2*$^{-/-}$ B cells.

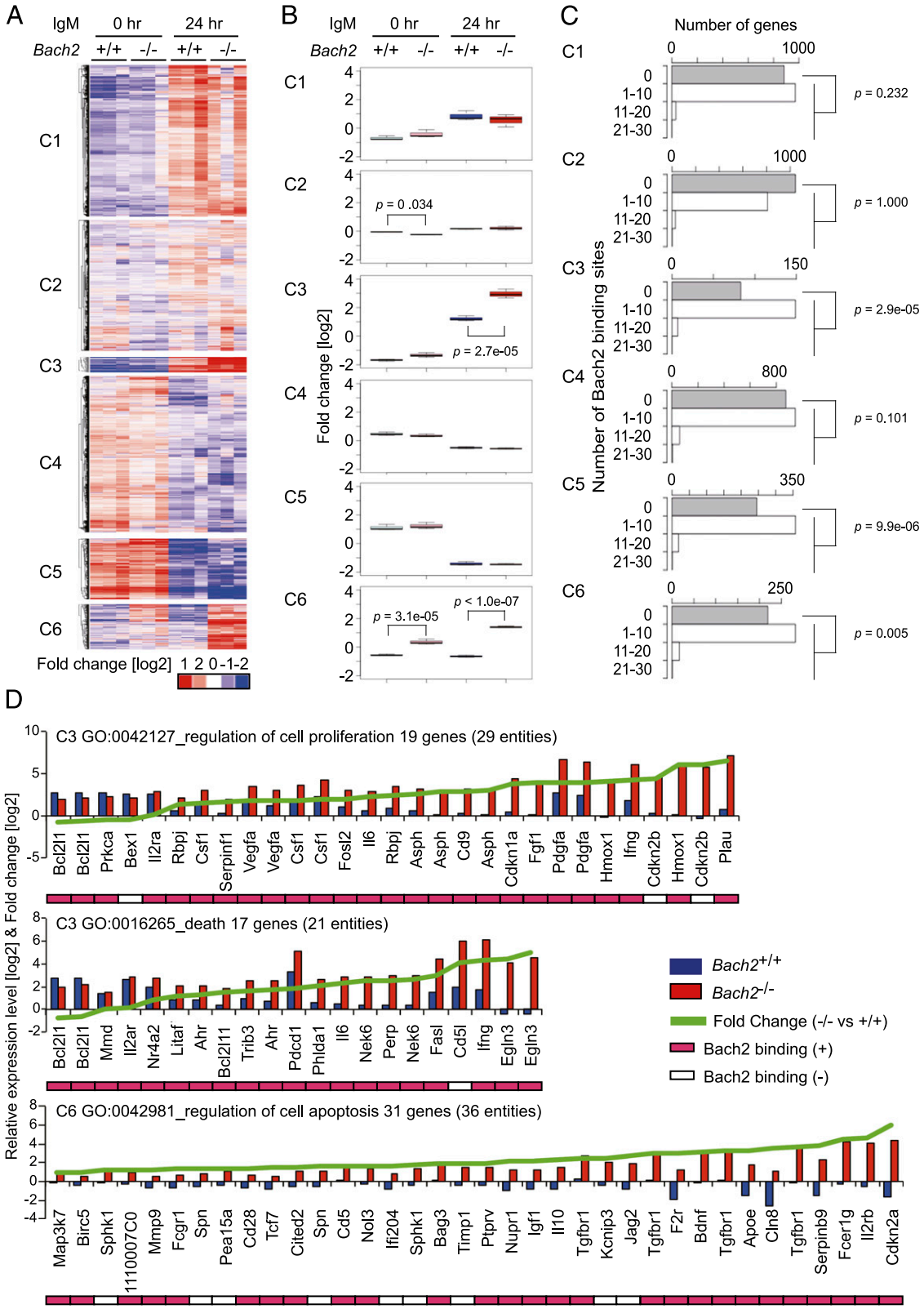

FIGURE 4. Comprehensive analysis of Bach2-dependent gene-expression signature in BCR-engaged B cells. (**A**) Global gene-expression profiles from DNA microarray analysis of WT and *Bach2*$^{-/-}$ FO B cells after BCR engagement for 24 h were subjected to k-means clustering. (**B**) Averaged gene-expression profiles of data shown in (A). Statistical difference between WT and *Bach2*$^{-/-}$ were assessed by the Tukey HSD test. (**C**) Enrichment of Bach2-bound genes in each cluster, assessed by the hypergeometric test. Bach2-bound genes were defined as genes harboring Bach2-binding peaks from ChIP-seq data within 50 kbp around the gene body. White and gray bars represent the number of genes with or without Bach2-binding peaks, respectively. (**D**) Bar graphs represent the relative mRNA expression in BCR-engaged B cells of the indicated genes assessed by DNA microarray analysis. Line graph represents the relative gene-expression levels in *Bach2*$^{-/-}$ FO B cells compared with WT FO B cells. Bach2-bound or unbound genes are represented by magenta or white boxes, respectively.

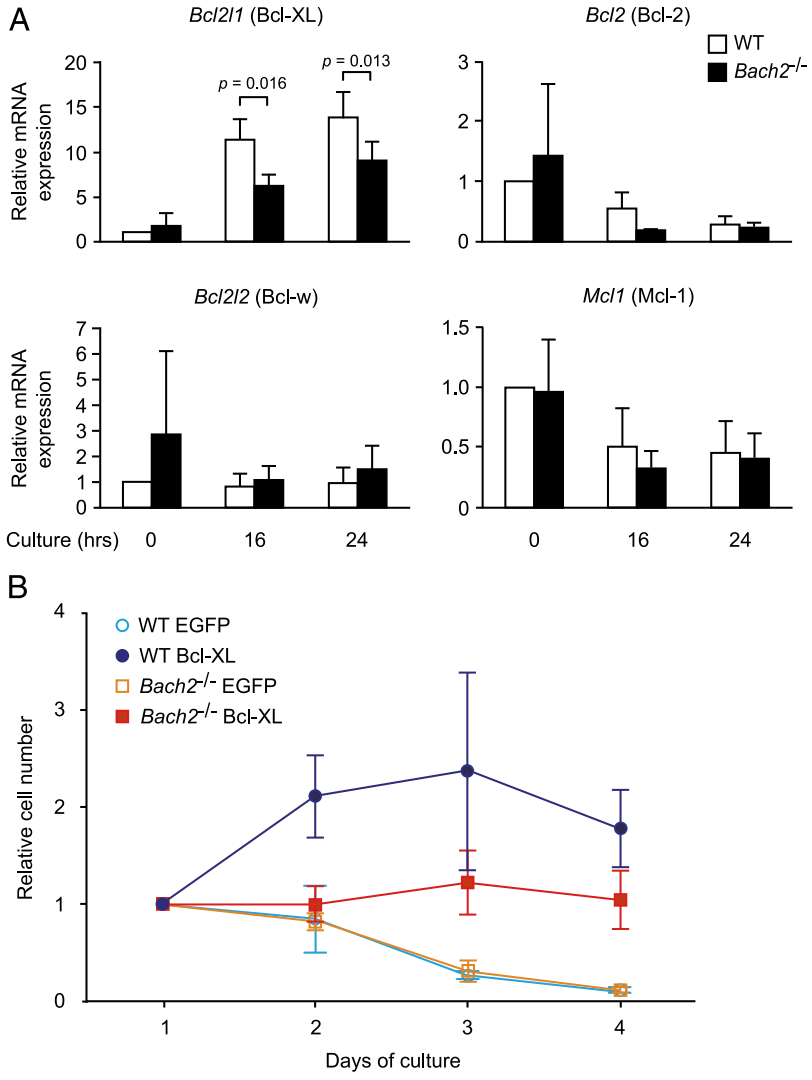

FIGURE 5. BCR-engaged *Bach2*$^{-/-}$ splenic B cells show reduced expression of Bcl-x_L. (**A**) mRNA expression levels of antiapoptotic Bcl-2 family members in WT and *Bach2*$^{-/-}$ splenic B cells, cultured in the presence of 10 μg/ml anti-IgM Ab for 0, 16, and 24 h, were measured by RT-qPCR. Expression levels were normalized to *β-actin* mRNA expression and then to the WT B cells 0-h sample. Data are the mean ± SD of three independent experiments. The *p* values were determined using a Student *t* test. (**B**) In vitro rescue experiments performed on splenic B cells isolated from WT or *Bach2*$^{-/-}$ mice. B cells were infected with a bicistronic retrovirus expressing Bcl-x_L and EGFP or a control retrovirus expressing EGFP. Infected B cells were cultured in the presence of 10 μg/ml anti-IgM Ab and harvested at the indicated time points. Cell viability was judged by EGFP expression using FACS. Relative cell numbers were calculated by normalization to the cell numbers at day 1 in each condition. Data are the mean ± SD of three independent experiments.

It has been reported that Bcl-x_L is required for B cell survival (54–56). Thus, it is possible that the reduced expression of *Bcl2l1* in *Bach2*$^{-/-}$ B cells is responsible for their impaired proliferation upon BCR signaling. Therefore, we investigated whether the proliferative defect in *Bach2*$^{-/-}$ B cells could be rescued by exogenous Bcl-x_L expression by transducing *Bach2*$^{-/-}$ splenic B cells with a bicistronic retrovirus expressing EGFP and Bcl-x_L or an EGFP-expressing control retrovirus. Cell proliferation is a prerequisite for efficient retroviral integration. Because *Bach2*$^{-/-}$ B cells proliferated poorly in response to BCR engagement (Fig. 1), proliferation of WT and *Bach2*$^{-/-}$ B cells was first induced with LPS for 24 h. After retroviral infection, B cells were stimulated by BCR engagement with anti-IgM Ab, and the fraction of EGFP$^+$ cells was measured every 24 h by flow cytometry. Unexpectedly, flow cytometric analysis showed that the percentages of cells infected with the control virus decreased in WT B cells, as well as B cells from *Bach2*$^{-/-}$ mice, following BCR engagement (Fig. 5B). It is possible that the viral infection procedure inhibited proliferation. Regardless of the genotype, the decrease in the relative numbers of B cells in response to BCR signaling was prevented when the cells were infected with the Bcl-x_L–expressing virus, indicating that Bcl-x_L inhibited apoptosis of the primary B cells. Notably, WT B cells showed a more vigorous response to the expression of Bcl-x_L than did *Bach2*$^{-/-}$ B cells. These results demonstrated that Bcl-x_L promoted the survival of BCR-stimulated B cells and that its overexpression in *Bach2*$^{-/-}$ B cells was not sufficient to fully restore the proliferation defect.

Overexpression of CKI genes in Bach2$^{-/-}$ *B cells*

Because the forced Bcl-x_L expression was insufficient to fully rescue the proliferation defect of *Bach2*$^{-/-}$ B cells, additional target genes of Bach2 must be responsible for this defect. Therefore, we focused on genes related to "regulation of cell proliferation" (GO:0042127) and "regulation of cell apoptosis" (GO:0042981) (Fig. 4D). Among these genes, transcript levels of CKI genes, such as *Cdkn1a*, *Cdkn2a*, and *Cdkn2b*, were highly upregulated in *Bach2*$^{-/-}$ B cells compared with WT B cells (Fig. 4D). Gene-expression analysis by RT-qPCR revealed that mRNA levels of *Cdkn1a* and *Cdkn2a* showed striking increases in response to BCR engagement in the absence of Bach2 (Fig. 6A). Similarly, an increase in *Cdkn1a* and *Cdkn2a* expression was observed in purified *Bach2*$^{-/-}$ FO B cells compared with WT FO B cells in response to BCR engagement (Supplemental Fig. 2B), indicating that altered expression was not simply due to the population difference between *Bach2*$^{-/-}$ and WT B220$^+$ B cells (20). In contrast, *Bach2*$^{-/-}$ and WT B cells displayed similar changes in *Cdkn1b* expression following BCR engagement. It has been reported that the *Cdkn1a* gene encoding p21 is directly activated by p53 (57); however, p53 expression was not elevated in *Bach2*$^{-/-}$ B cells (Supplemental Fig. 2C), indicating that the elevated mRNA level of *Cdkn1a* was not due to excessive induction of p53 levels in *Bach2*$^{-/-}$ B cells. In contrast to CKI genes, we did not observe significant changes in the expression levels of

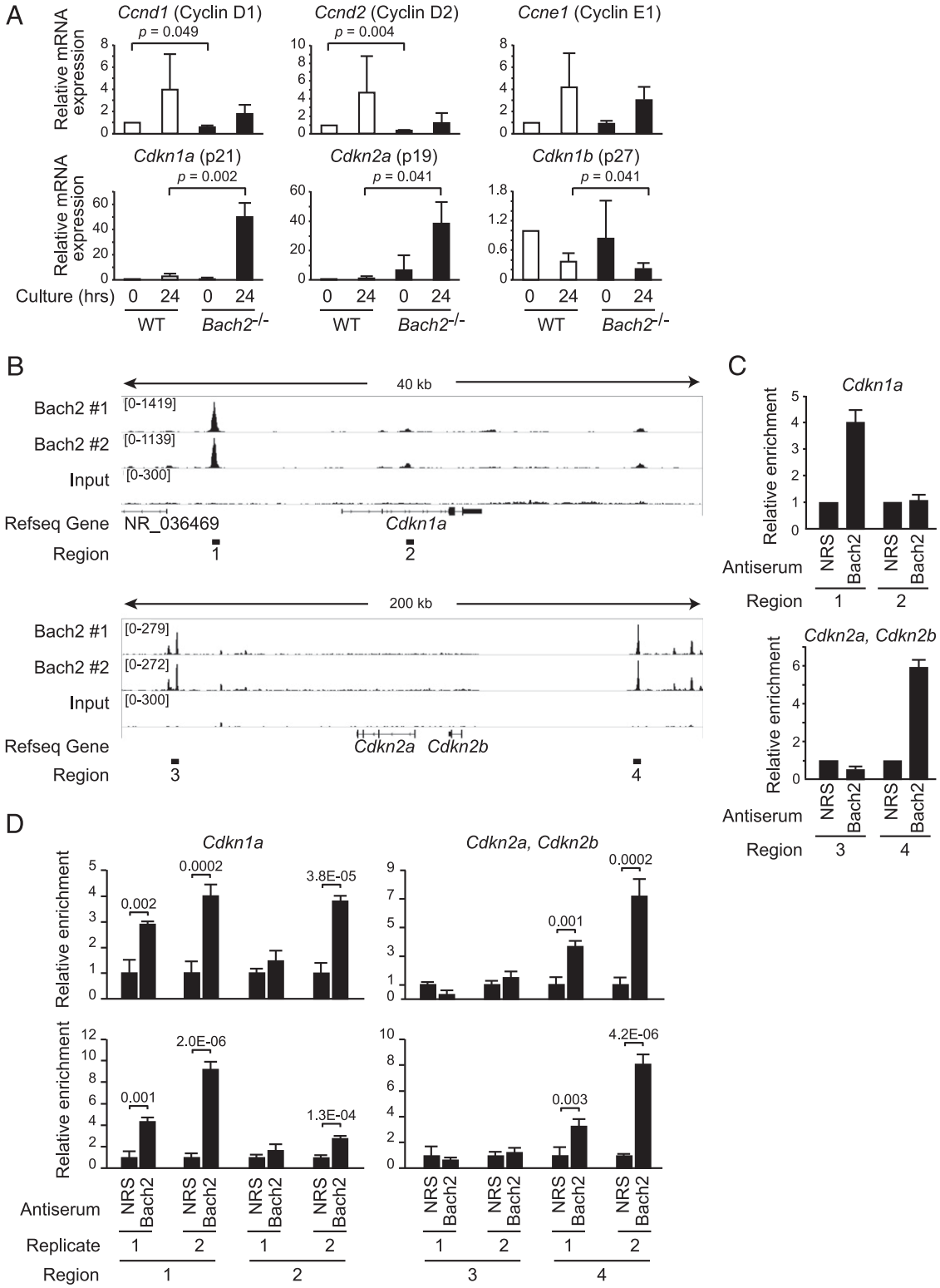

FIGURE 6. CKI genes are newly identified Bach2 direct target genes. (**A**) mRNA expression of regulators of the transition from the G_1 phase to the S phase of the cell cycle in WT and *Bach2*$^{-/-}$ splenic B cells, cultured with 10 μg/ml anti-IgM Ab for 0 and 24 h, was measured by RT-qPCR. Results were normalized to the levels of *β-actin* mRNA and then to WT B cells at 0 h. Data are the mean ± SD of three independent experiments. (**B**) ChIP-seq analysis of the binding of Bach2 across the *Cdkn1a*, *Cdkn2a*, and *Cdkn2b* loci in the *Ebf1*$^{-/-}$ pre–pro-B cell line. Data are from two independent ChIP-seq experiments. Tracks of input DNA used in the ChIP assay are also indicated. Numbers in the upper left corners indicate the range of sequence tags for each track. The exon–intron structure, according to the RefSeq database, is shown under each panel; arrowheads indicate the direction of transcription. Region numbers indicate the loci that were investigated in (**C**) and (**D**). (C) Binding of Bach2 to the *Cdkn1a* (upper panel) and *Cdk2a* and *Cdkn2b* (lower panel) loci was demonstrated by ChIP-qPCR in the BAL17 mature B cell line. Results are shown as enrichment relative to sample immunoprecipitated by NRS. (D) Binding of Bach2 to the *Cdkn1a* (left panels) and *Cdkn2b* (right panels) loci was confirmed by ChIP-qPCR in WT and *Bach2*$^{-/-}$ splenic B cells before and after BCR engagement for 24 h. Results are shown as enrichment relative to sample immunoprecipitated by NRS. Data are the mean ± SD. The *p* values were determined using a Student *t* test.

Ccnd1, *Ccnd2*, or other cyclin genes that could account for the proliferation defect in of *Bach2*$^{-/-}$ B cells (Fig. 6A). Moreover, there was no significant difference between *Bach2*$^{-/-}$ and WT B cells with regard to the expression levels of CDK genes, such as *Cdk2* and *Cdk10* (Supplemental Fig. 2D).

Direct regulation of CKI genes by Bach2

To investigate whether Bach2 mediates transcriptional repression by directly binding to the *Cdkn1a* and *Cdkn2b* loci in B cells, we further analyzed the aforementioned ChIP-seq data. Bach2-binding peaks were found near *Cdkn1a* and *Cdkn2b* (Fig. 6B). Binding of Bach2 to these regions was validated by ChIP followed by quantitative PCR (ChIP-qPCR) using BAL17 B cells (Fig. 6C). We observed that Bach2 specifically binds to several regions in proximity to *Cdkn1a* and *Cdkn2b* loci. Bach2 binding to the other regions could not be detected in BAL17 mature B cells (Fig. 6C). Similar results were obtained by ChIP-qPCR experiments in mice splenic B cells before and after BCR engagement (Fig. 6D). Collectively, these data suggest that Bach2 directly represses the expression of *Cdkn1a*, *Cdkn2a*, and *Cdkn2b* genes in BCR-engaged B cells to promote cell cycle progression.

Discussion

Mature B cells exhibit a remarkable control of their proliferative rate in response to extrinsic signals, disorders of which often lead to malignant transformation (9). Mature B cells remain dormant in the peripheral lymphoid tissues but, upon Ag encounter, they undergo massive clonal expansion (5). Furthermore, CSR requires multiple proteins in the DNA damage response pathway that connects damage sensing, repair, and transient inhibition of DNA replication (58). As such, proliferation of mature B cells must be tightly controlled. Our study of the proliferation defect of *Bach2*$^{-/-}$ B cells upon BCR signaling has elucidated an important transcriptional mechanism governing cell cycle progression and survival that is regulated by Bach2. We found that ablation of the *Bach2* gene resulted in reduced cell cycle progression and increased apoptosis upon BCR signaling. Antiapoptotic factor Bcl-x_L partially rescued the cell-proliferation defect in *Bach2*$^{-/-}$ B cells. We have further identified CKI genes *Cdkn1a*, *Cdkn2a*, and *Cdkn2b* as direct target genes of Bach2. Collectively, these results suggest that induction of the Bcl-x_L expression and repression of CKI genes by Bach2 constitutes an indispensable regulatory network for B cell proliferation in response to BCR signaling.

One of the well-established regulatory networks for cell proliferation of mature B cells involves *Prdm1* and *Myc*. *Myc* drives proliferation of activated B cells, whereas *Prdm1* inhibits proliferation by repressing *Myc* (59–61). However, although *Bach2*$^{-/-}$ B cells proliferated vigorously in response to LPS, removal of *Prdm1* from *Bach2*$^{-/-}$ B cells results in a reduction in cell proliferation in response to LPS (21), suggesting that Bach2 constitutes an important regulator of cell proliferation in parallel with *Prdm1*. The results of this study suggest that Bach2 promotes proliferation of activated B cells by repressing the expression of CKI genes, as well as *Prdm1*.

Recently, we have reported that Bach2 is phosphorylated in response to BCR stimulation by the PI3K–Akt–mTOR signaling pathway. Phosphorylation of Bach2 results in inhibition of its nuclear accumulation and loss of its activity as a transcriptional repressor (32). Additionally, the PI3K–Akt–mTOR signaling pathway downregulates transcription of *Bach2* in B cells (32). Therefore, it appears to be a conundrum that Bach2 activity is inhibited at multiple levels by the BCR signaling pathway, despite promoting cell cycle progression and survival in response to BCR signaling. One interesting possibility is that its target genes, such as *Cdkn1a*, may acquire epigenetic histone modifications for repression, depending on Bach2 prior to BCR stimulation. This idea is supported by our recent observation that Bach2 forms a protein complex with histone deacetylase 3 and promotes histone deacetylation to repress *Prdm1* (29). Inefficient epigenetic repression of CKI genes in *Bach2*$^{-/-}$ B cells may lead to their rapid induction upon BCR stimulation. In WT B cells, these target genes may remain epigenetically repressed for some time, even when Bach2 is inactivated by the BCR–PI3K–Akt–mTOR pathway. When PCs stop proliferating, CKI genes may finally be induced by histone acetylation.

For successful SHM and CSR in GC B cells, cells need to suppress apoptosis and arrest their cell cycle while the induced DNA damage is repaired. Several studies have suggested mechanisms that prevent apoptosis in GC B cells (13, 62). It has been reported that cooperation between Bach2 and Bcl6 is indispensable for the GC response (31, 46). Bcl6 has been shown to directly repress DNA damage-sensing and checkpoint genes, such as *TP53* encoding p53 (13), allowing GC B cells to keep proliferating under conditions of frequent DNA damage introduced by activation-induced cytidine deaminase. Our results suggest that Bach2 is another critical regulator of cell cycle arrest and proliferation in GC B cells. Although p53 expression was not affected by the absence of Bach2, we found direct repression of CKI genes by Bach2. Previous reports have shown that Bcl6 also directly represses some of these CKI genes (*Cdkn1a*, *Cdkn1b*, *Cdkn2a*, and *Cdkn2b*) (46, 62, 63). However, considering the prominent induction of CKI genes in *Bach2*$^{-/-}$ B cells, Bach2 may play the dominant role in the repression of CKI genes in activated B cells. An interesting question emerging from this study is whether Bach2 is involved in the switching of cell cycle arrest and reproliferation among GC B cells.

Our results and previous studies suggest that Bcl6 and Bach2 regulate apoptosis in opposite directions. Bcl6 represses the expression of Bcl-2, a key antiapoptotic factor, limiting cell survival in GC B cells and, thereby, preventing tumorigenesis (63, 64). In contrast, Bach2 is required to induce sufficient expression of *Bcl2l1* mRNA, which encodes Bcl-x_L, and to suppress apoptosis. Collectively, Bach2 and Bcl6 may not only cooperate to promote cell cycle progression, they also regulate different pathways governing DNA damage response and cell survival of mature B cells. Bcl-x_L has been linked to the clonal selection and suppression of apoptosis of GC B cells in response to Ag (54–56). Taken together with these previous reports, our observations suggest that Bach2-dependent Bcl-x_L expression may be important for clonal selection during B cell differentiation and for GC formation. One of the remaining questions is how Bach2 promotes the expression of Bcl-x_L. Because Bcl-x_L is directly activated by NF-κB in response to BCR engagement (56), Bach2 may affect the expression of genes critical for the NF-κB pathway.

Although expression of *Bcl2l1* mRNA is decreased significantly among FACS-sorted FO B cells and bulk B cells from *Bach2*$^{-/-}$ mice (Figs. 4D, 5A, Supplemental Fig. 2A), differences among unfractionated B cell populations were attenuated when purified FO B cells were analyzed. It is possible that differences in the underlying frequency of distinct B cell subpopulations in spleens of WT and *Bach2*$^{-/-}$ mice, as well as differing expression of *Bcl2l1* mRNA within these subsets, contribute to more substantial differences when bulk unfractionated populations are analyzed. Alternatively, the effect of Bach2 on *Bcl2l1* mRNA expression may be less pronounced among FO B cells than within the variety of B cell subsets in the spleen.

Our findings that Bach2 promotes cell cycle progression and survival upon BCR signaling will shed light on the pathogenic

mechanisms of lymphomagenesis/leukemogenesis associated with *BACH2* aberrations. *BACH2* has been identified as a partner gene of IgH (*IGH*) translocation among B cell lymphoma/leukemia patients carrying *IGH/MYC* translocation (40). This dual translocation leads to high levels of *BACH2* expression and was linked to an aggressive phenotype. Furthermore, we have recently reported that *BACH2* expression can be used as a predictive marker of diffuse large B cell lymphoma (38). Diffuse large B cell lymphoma patients with high BACH2 expression have a shorter 3-y overall survival rate than those with low BACH2 expression. Our observations in this study predict that high levels of BACH2 expression may sustain cell cycle progression, as well as suppress apoptosis, leading to an aggressive cancer phenotype; however, several clinical reports proposed that BACH2 functions as a tumor suppressor (39, 65, 66). For example, mutations in *BACH2* are found in pre-B cell leukemia, resulting in a failure of p53-dependent apoptosis (66). Perhaps the tumor-promoting or -suppressing role of Bach2 depends on the stages of B cell differentiation of the cell of origin. Therefore, identifying downstream target genes of Bach2 and the regulatory cascade of Bach2 activity at each stage of B cell development will contribute to an understanding of the regulation of cell proliferation during B cell development and its deregulation in malignant B cell transformation.

Acknowledgments

We thank members of the Igarashi laboratory for helpful discussions; Dr. T. Kurosaki and Dr. K. Kometani (RIKEN) for discussions; M. Tsuda, M. Kikuchi, M. Nakagawa, and K. Kuroda for technical assistance; and the Biomedical Research Core of Tohoku University Graduate School of Medicine for technical support.

Disclosures

The authors have no financial conflicts of interest.

References

1. Bianconi, E., A. Piovesan, F. Facchin, A. Beraudi, R. Casadei, F. Frabetti, L. Vitale, M. C. Pelleri, S. Tassani, F. Piva, et al. 2013. An estimation of the number of cells in the human body. *Ann. Hum. Biol.* 40: 463–471.
2. Sender, R., S. Fuchs, and R. Milo. 2016. Revised estimates for the number of human and bacteria cells in the body. *PLoS Biol.* 14: e1002533.
3. Sun, J., A. Ramos, B. Chapman, J. B. Johnnidis, L. Le, Y. J. Ho, A. Klein, O. Hofmann, and F. D. Camargo. 2014. Clonal dynamics of native haematopoiesis. *Nature* 514: 322–327.
4. Hardy, R. R., C. E. Carmack, S. A. Shinton, J. D. Kemp, and K. Hayakawa. 1991. Resolution and characterization of pro-B and pre-pro-B cell stages in normal mouse bone marrow. *J. Exp. Med.* 173: 1213–1225.
5. Jacob, J., R. Kassir, and G. Kelsoe. 1991. In situ studies of the primary immune response to (4-hydroxy-3-nitrophenyl)acetyl. I. The architecture and dynamics of responding cell populations. *J. Exp. Med.* 173: 1165–1175.
6. Muramatsu, M., H. Nagaoka, R. Shinkura, N. A. Begum, and T. Honjo. 2007. Discovery of activation-induced cytidine deaminase, the engraver of antibody memory. *Adv. Immunol.* 94: 1–36.
7. Schamel, W. W., and M. Reth. 2000. Monomeric and oligomeric complexes of the B cell antigen receptor. *Immunity* 13: 5–14.
8. De Silva, N. S., and U. Klein. 2015. Dynamics of B cells in germinal centres. *Nat. Rev. Immunol.* 15: 137–148.
9. Basso, K., and R. Dalla-Favera. 2015. Germinal centres and B cell lymphomagenesis. *Nat. Rev. Immunol.* 15: 172–184.
10. Corcoran, L. M., and D. M. Tarlinton. 2016. Regulation of germinal center responses, memory B cells and plasma cell formation-an update. *Curr. Opin. Immunol.* 39: 59–67.
11. Ramiro, A. R., M. Jankovic, E. Callen, S. Difilippantonio, H. T. Chen, K. M. McBride, T. R. Eisenreich, J. Chen, R. A. Dickins, S. W. Lowe, et al. 2006. Role of genomic instability and p53 in AID-induced c-myc-Igh translocations. *Nature* 440: 105–109.
12. Mailand, N., J. Falck, C. Lukas, R. G. Syljuâsen, M. Welcker, J. Bartek, and J. Lukas. 2000. Rapid destruction of human Cdc25A in response to DNA damage. *Science* 288: 1425–1429.
13. Phan, R. T., and R. Dalla-Favera. 2004. The BCL6 proto-oncogene suppresses p53 expression in germinal-centre B cells. *Nature* 432: 635–639.
14. Ranuncolo, S. M., L. Wang, J. M. Polo, T. Dell'Oso, J. Dierov, T. J. Gaymes, F. Rassool, M. Carroll, and A. Melnick. 2008. BCL6-mediated attenuation of DNA damage sensing triggers growth arrest and senescence through a p53-dependent pathway in a cell context-dependent manner. *J. Biol. Chem.* 283: 22565–22572.
15. Gitlin, A. D., Z. Shulman, and M. C. Nussenzweig. 2014. Clonal selection in the germinal centre by regulated proliferation and hypermutation. *Nature* 509: 637–640.
16. Kallies, A., J. Hasbold, D. M. Tarlinton, W. Dietrich, L. M. Corcoran, P. D. Hodgkin, and S. L. Nutt. 2004. Plasma cell ontogeny defined by quantitative changes in blimp-1 expression. *J. Exp. Med.* 200: 967–977.
17. Richards, S., C. Watanabe, L. Santos, A. Craxton, and E. A. Clark. 2008. Regulation of B-cell entry into the cell cycle. *Immunol. Rev.* 224: 183–200.
18. Igarashi, K., and A. Itoh-Nakadai. 2016. Orchestration of B lymphoid cells and their inner myeloid by Bach. *Curr. Opin. Immunol.* 39: 136–142.
19. Itoh-Nakadai, A., R. Hikota, A. Muto, K. Kometani, M. Watanabe-Matsui, Y. Sato, M. Kobayashi, A. Nakamura, Y. Miura, Y. Yano, et al. 2014. The transcription repressors Bach2 and Bach1 promote B cell development by repressing the myeloid program. *Nat. Immunol.* 15: 1171–1180.
20. Muto, A., S. Tashiro, O. Nakajima, H. Hoshino, S. Takahashi, E. Sakoda, D. Ikebe, M. Yamamoto, and K. Igarashi. 2004. The transcriptional programme of antibody class switching involves the repressor Bach2. *Nature* 429: 566–571.
21. Muto, A., K. Ochiai, Y. Kimura, A. Itoh-Nakadai, K. L. Calame, D. Ikebe, S. Tashiro, and K. Igarashi. 2010. Bach2 represses plasma cell gene regulatory network in B cells to promote antibody class switch. *EMBO J.* 29: 4048–4061.
22. Roychoudhuri, R., K. Hirahara, K. Mousavi, D. Clever, C. A. Klebanoff, M. Bonelli, G. Sciumè, H. Zare, G. Vahedi, B. Dema, et al. 2013. BACH2 represses effector programs to stabilize T(reg)-mediated immune homeostasis. *Nature* 498: 506–510.
23. Roychoudhuri, R., D. Clever, P. Li, Y. Wakabayashi, K. M. Quinn, C. A. Klebanoff, Y. Ji, M. Sukumar, R. L. Eil, Z. Yu, et al. 2016. BACH2 regulates CD8(+) T cell differentiation by controlling access of AP-1 factors to enhancers. *Nat. Immunol.* 17: 851–860.
24. Tsukumo, S., M. Unno, A. Muto, A. Takeuchi, K. Kometani, T. Kurosaki, K. Igarashi, and T. Saito. 2013. Bach2 maintains T cells in a naive state by suppressing effector memory-related genes. *Proc. Natl. Acad. Sci. USA* 110: 10735–10740.
25. Kim, E. H., D. J. Gasper, S. H. Lee, E. H. Plisch, J. Svaren, and M. Suresh. 2014. Bach2 regulates homeostasis of Foxp3+ regulatory T cells and protects against fatal lung disease in mice. *J. Immunol.* 192: 985–995.
26. Kuwahara, M., J. Suzuki, S. Tofukuji, T. Yamada, M. Kanoh, A. Matsumoto, S. Maruyama, K. Kometani, T. Kurosaki, O. Ohara, et al. 2014. The Menin-Bach2 axis is critical for regulating CD4 T-cell senescence and cytokine homeostasis. *Nat. Commun.* 5: 3555.
27. Ebina-Shibuya, R., M. Watanabe-Matsui, M. Matsumoto, A. Itoh-Nakadai, R. Funayama, K. Nakayama, A. Muto, and K. Igarashi. 2016. The double knockout of Bach1 and Bach2 in mice reveals shared compensatory mechanisms in regulating alveolar macrophage function and lung surfactant homeostasis. *J. Biochem.* 160: 333–344.
28. Nakamura, A., R. Ebina-Shibuya, A. Itoh-Nakadai, A. Muto, H. Shima, D. Saigusa, J. Aoki, M. Ebina, T. Nukiwa, and K. Igarashi. 2013. Transcription repressor Bach2 is required for pulmonary surfactant homeostasis and alveolar macrophage function. *J. Exp. Med.* 210: 2191–2204.
29. Tanaka, H., A. Muto, H. Shima, Y. Katoh, N. Sax, S. Tajima, A. Brydun, T. Ikura, N. Yoshizawa, H. Masai, et al. 2016. Epigenetic regulation of the Blimp-1 gene (Prdm1) in B cells involves Bach2 and histone deacetylase 3. *J. Biol. Chem.* 291: 6316–6330.
30. Ochiai, K., Y. Katoh, T. Ikura, Y. Hoshikawa, T. Noda, H. Karasuyama, S. Tashiro, A. Muto, and K. Igarashi. 2006. Plasmacytic transcription factor Blimp-1 is repressed by Bach2 in B cells. *J. Biol. Chem.* 281: 38226–38234.
31. Ochiai, K., A. Muto, H. Tanaka, S. Takahashi, and K. Igarashi. 2008. Regulation of the plasma cell transcription factor Blimp-1 gene by Bach2 and Bcl6. *Int. Immunol.* 20: 453–460.
32. Ando, R., H. Shima, T. Tamahara, Y. Sato, M. Watanabe-Matsui, H. Kato, N. Sax, H. Motohashi, K. Taguchi, M. Yamamoto, et al. 2016. The transcription factor Bach2 is phosphorylated at multiple sites in murine B cells but a single site prevents its nuclear localization. *J. Biol. Chem.* 291: 1826–1840.
33. Srinivasan, L., Y. Sasaki, D. P. Calado, B. Zhang, J. H. Paik, R. A. DePinho, J. L. Kutok, J. F. Kearney, K. L. Otipoby, and K. Rajewsky. 2009. PI3 kinase signals BCR-dependent mature B cell survival. *Cell* 139: 573–586.
34. Werner, M., E. Hobeika, and H. Jumaa. 2010. Role of PI3K in the generation and survival of B cells. *Immunol. Rev.* 237: 55–71.
35. Gold, M. R., M. P. Scheid, L. Santos, M. Dang-Lawson, R. A. Roth, L. Matsuuchi, V. Duronio, and D. L. Krebs. 1999. The B cell antigen receptor activates the Akt (protein kinase B)/glycogen synthase kinase-3 signaling pathway via phosphatidylinositol 3-kinase. *J. Immunol.* 163: 1894–1905.
36. Sears, R., F. Nuckolls, E. Haura, Y. Taya, K. Tamai, and J. R. Nevins. 2000. Multiple Ras-dependent phosphorylation pathways regulate Myc protein stability. *Genes Dev.* 14: 2501–2514.
37. Sears, R. C., and J. R. Nevins. 2002. Signaling networks that link cell proliferation and cell fate. *J. Biol. Chem.* 277: 11617–11620.
38. Ichikawa, S., N. Fukuhara, H. Katsushima, T. Takahashi, J. Yamamoto, H. Yokoyama, O. Sasaki, O. Fukuhara, J. Nomura, K. Ishizawa, et al. 2014. Association between BACH2 expression and clinical prognosis in diffuse large B-cell lymphoma. *Cancer Sci.* 105: 437–444.
39. Sakane-Ishikawa, E., S. Nakatsuka, Y. Tomita, S. Fujita, I. Nakamichi, T. Takakuwa, H. Sugiyama, S. Fukuhara, M. Hino, A. Kanamaru, et al; Osaka Lymphoma Study Group. 2005. Prognostic significance of BACH2 expression in diffuse large B-cell lymphoma: a study of the Osaka Lymphoma Study Group. *J. Clin. Oncol.* 23: 8012–8017.

40. Kobayashi, S., T. Taki, Y. Chinen, Y. Tsutsumi, M. Ohshiro, T. Kobayashi, Y. Matsumoto, J. Kuroda, S. Horiike, K. Nishida, and M. Taniwaki. 2011. Identification of IGHCδ-BACH2 fusion transcripts resulting from cryptic chromosomal rearrangements of 14q32 with 6q15 in aggressive B-cell lymphoma/leukemia. *Genes Chromosomes Cancer* 50: 207–216.
41. Rad, R., L. Rad, W. Wang, J. Cadinanos, G. Vassiliou, S. Rice, L. S. Campos, K. Yusa, R. Banerjee, M. A. Li, et al. 2010. PiggyBac transposon mutagenesis: a tool for cancer gene discovery in mice. *Science* 330: 1104–1107.
42. Dennis, , G., Jr., B. T. Sherman, D. A. Hosack, J. Yang, W. Gao, H. C. Lane, and R. A. Lempicki. 2003. DAVID: database for annotation, visualization, and integrated discovery. *Genome Biol.* 4: P3.
43. Muto, A., S. Tashiro, H. Tsuchiya, A. Kume, M. Kanno, E. Ito, M. Yamamoto, and K. Igarashi. 2002. Activation of Maf/AP-1 repressor Bach2 by oxidative stress promotes apoptosis and its interaction with promyelocytic leukemia nuclear bodies. *J. Biol. Chem.* 277: 20724–20733.
44. Shinnakasu, R., T. Inoue, K. Kometani, S. Moriyama, Y. Adachi, M. Nakayama, Y. Takahashi, H. Fukuyama, T. Okada, and T. Kurosaki. 2016. Regulated selection of germinal-center cells into the memory B cell compartment. *Nat. Immunol.* 17: 861–869.
45. Nakayama, Y., P. Stabach, S. E. Maher, M. C. Mahajan, P. Masiar, C. Liao, X. Zhang, Z. J. Ye, D. Tuck, A. L. Bothwell, et al. 2006. A limited number of genes are involved in the differentiation of germinal center B cells. *J. Cell. Biochem.* 99: 1308–1325.
46. Huang, C., H. Geng, I. Boss, L. Wang, and A. Melnick. 2014. Cooperative transcriptional repression by BCL6 and BACH2 in germinal center B-cell differentiation. *Blood* 123: 1012–1020.
47. Lecoeur, H., E. Ledru, M. C. Prévost, and M. L. Gougeon. 1997. Strategies for phenotyping apoptotic peripheral human lymphocytes comparing ISNT, annexin-V and 7-AAD cytofluorometric staining methods. *J. Immunol. Methods* 209: 111–123.
48. Andjelic, S., and H. C. Liou. 1998. Antigen receptor-induced B lymphocyte apoptosis mediated via a protease of the caspase family. *Eur. J. Immunol.* 28: 570–581.
49. Mack, A., C. Fürmann, and G. Häcker. 2000. Detection of caspase-activation in intact lymphoid cells using standard caspase substrates and inhibitors. *J. Immunol. Methods* 241: 19–31.
50. Itoh-Nakadai, A., M. Matsumoto, H. Kato, J. Sasaki, Y. Uehara, Y. Sato, R. Ebina-Shibuya, M. Morooka, R. Funayama, K. Nakayama, et al. 2017. A Bach2-Cebp gene regulatory network for the commitment of multipotent hematopoietic progenitors. *Cell Rep.* 18: 2401–2414.
51. Adams, J. M., and S. Cory. 2007. Bcl-2-regulated apoptosis: mechanism and therapeutic potential. *Curr. Opin. Immunol.* 19: 488–496.
52. Eeva, J., U. Nuutinen, A. Ropponen, M. Mättö, M. Eray, R. Pellinen, J. Wahlfors, and J. Pelkonen. 2009. Feedback regulation of mitochondria by caspase-9 in the B cell receptor-mediated apoptosis. *Scand. J. Immunol.* 70: 574–583.
53. Lee, H. H., H. Dadgostar, Q. Cheng, J. Shu, and G. Cheng. 1999. NF-kappaB-mediated up-regulation of Bcl-x and Bfl-1/A1 is required for CD40 survival signaling in B lymphocytes. *Proc. Natl. Acad. Sci. USA* 96: 9136–9141.
54. Takahashi, Y., D. M. Cerasoli, J. M. Dal Porto, M. Shimoda, R. Freund, W. Fang, D. G. Telander, E. N. Malvey, D. L. Mueller, T. W. Behrens, and G. Kelsoe. 1999. Relaxed negative selection in germinal centers and impaired affinity maturation in bcl-xL transgenic mice. *J. Exp. Med.* 190: 399–410.
55. Grillot, D. A., R. Merino, J. C. Pena, W. C. Fanslow, F. D. Finkelman, C. B. Thompson, and G. Nunez. 1996. bcl-x exhibits regulated expression during B cell development and activation and modulates lymphocyte survival in transgenic mice. *J. Exp. Med.* 183: 381–391.
56. Cheng, S., C. Y. Hsia, G. Leone, and H. C. Liou. 2003. Cyclin E and Bcl-xL cooperatively induce cell cycle progression in c-Rel$^{-/-}$ B cells. *Oncogene* 22: 8472–8486.
57. Löhr, K., C. Möritz, A. Contente, and M. Dobbelstein. 2003. p21/CDKN1A mediates negative regulation of transcription by p53. *J. Biol. Chem.* 278: 32507–32516.
58. Franco, S., F. W. Alt, and J. P. Manis. 2006. Pathways that suppress programmed DNA breaks from progressing to chromosomal breaks and translocations. *DNA Repair (Amst.)* 5: 1030–1041.
59. Dominguez-Sola, D., G. D. Victora, C. Y. Ying, R. T. Phan, M. Saito, M. C. Nussenzweig, and R. Dalla-Favera. 2012. The proto-oncogene MYC is required for selection in the germinal center and cyclic reentry. *Nat. Immunol.* 13: 1083–1091.
60. Calado, D. P., Y. Sasaki, S. A. Godinho, A. Pellerin, K. Köchert, B. P. Sleckman, I. M. de Alborán, M. Janz, S. Rodig, and K. Rajewsky. 2012. The cell-cycle regulator c-Myc is essential for the formation and maintenance of germinal centers. *Nat. Immunol.* 13: 1092–1100.
61. Lin, Y., K. Wong, and K. Calame. 1997. Repression of c-myc transcription by Blimp-1, an inducer of terminal B cell differentiation. *Science* 276: 596–599.
62. Phan, R. T., M. Saito, K. Basso, H. Niu, and R. Dalla-Favera. 2005. BCL6 interacts with the transcription factor Miz-1 to suppress the cyclin-dependent kinase inhibitor p21 and cell cycle arrest in germinal center B cells. *Nat. Immunol.* 6: 1054–1060.
63. Ci, W., J. M. Polo, L. Cerchietti, R. Shaknovich, L. Wang, S. N. Yang, K. Ye, P. Farinha, D. E. Horsman, R. D. Gascoyne, et al. 2009. The BCL6 transcriptional program features repression of multiple oncogenes in primary B cells and is deregulated in DLBCL. *Blood* 113: 5536–5548.
64. Saito, M., U. Novak, E. Piovan, K. Basso, P. Sumazin, C. Schneider, M. Crespo, Q. Shen, G. Bhagat, A. Califano, et al. 2009. BCL6 suppression of BCL2 via Miz1 and its disruption in diffuse large B cell lymphoma. *Proc. Natl. Acad. Sci. USA* 106: 11294–11299.
65. Green, M., M. K. Gandhi, E. Camilleri, P. Marlton, R. Lea, and L. Griffiths. 2009. High levels of BACH2 associated with lower levels of BCL2 transcript abundance in t(14;18)(q21;q34) translocation positive non-Hodgkin's lymphoma. *Leuk. Res.* 33: 731–734.
66. Swaminathan, S., C. Huang, H. Geng, Z. Chen, R. Harvey, H. Kang, C. Ng, B. Titz, C. Hurtz, M. F. Sadiyah, et al. 2013. BACH2 mediates negative selection and p53-dependent tumor suppression at the pre-B cell receptor checkpoint. *Nat. Med.* 19: 1014–1022.